LIGO-P070053-00-Z

LIGO's Search for Gravitational Waves from Binary Neutron Stars

Warren G. Anderson[1] and Jolien D. E. Creighton[2]

[1] Department of Physics, University of Wisconsin – Milwaukee, P.O. Box 413, Milwaukee, Wisconsin, 53201-0413, U.S.A. warren@gravity.phys.uwm.edu
[2] Department of Physics, University of Wisconsin – Milwaukee, P.O. Box 413, Milwaukee, Wisconsin, 53201-0413, U.S.A. jolien@gravity.phys.uwm.edu

Summary. The Laser Interferometer Gravitational-wave Observatory (LIGO) is one of a new generation of observatories looking for gravitational waves. These waves, emitted by highly relativistic systems, will open a new window for observation of the cosmos when they are detected. Among the most promising sources of gravitational waves for LIGO are compact binaries in the final minutes before coalescence. In this article, we review in brief the theory, methods, and results of LIGO's search for gravitational waves from neutron star binaries. No detections have been made to date. However, the best direct observational limits on coalesence rates have been set. The instrumentation and analysis methods, many of which were pioneered by the LIGO Scientific Collaboration, continue to be refined toward the ultimate goal of defining the new field of gravitational wave astronomy.

1 Introduction

The Laser Interferometer Gravitational-wave Observatory, or LIGO [1, 2] is one of the new generation of interferometric observatories for gravitational waves [3] which have come into operation over the last decade. LIGO consists of three interferometers – one with 4 km arms and another with 2 km arms housed in the same enclosure near Hanford, Washington (denoted by H1 and H2 respectively), and another with 4 km arms near Livingston Louisiana (denoted by L1). Currently, they are the most sensitive gravitational wave detectors in the world.

There are four categories of gravitational wave signals which LIGO is currently trying to detect: quasi-periodic signals, such as those expected from pulsars [4, 5, 6, 7, 8], stochastic background signals, such as remnant gravitational waves from the Big Bang [9, 10, 11, 12, 13], unmodeled burst signals, such as those that might be emitted by supernovae [14, 15, 16, 17, 18, 19], and inspiral signals, such as those from neutron star or black hole binaries [20, 21, 22, 23, 24]. In this article, we will only be concerned with the

last of these searches, and in particular the search for neutron star binaries [20, 23, 24].

This article is organized as follows: Since many astronomers may not be very familiar with gravitational waves and the effort to use them for astronomy, Sect. 2 is devoted to background material. This includes a simple description of what gravitational waves are and how they are generated, a brief history of the instruments and efforts to detect them, and some background on the relevant aspects of neutron star binaries and the gravitational waves they produce. Section 3 describes in some detail how LIGO searches for gravitational waves from neutron star binaries, including a description of the data, the data analysis methods employed, and coincidence vetoes.

Section 4 is devoted to results. In particular, it reports the published upper limits that LIGO has placed on the rate of neutron star binary coalescence in our galactic neighborhood. Also included is a description of the statistical analysis used to place these upper limits. In Sect. 5, we discuss prospects for better upper limits and discuss some of the astrophysics that might be done by LIGO when it reaches a sensitivity where gravitational waves from neutron star binaries are regularly observed. Concluding remarks are found in Sect. 6.

2 Background

2.1 Gravitational Waves

One of the many remarkable predictions of Einstein's general theory of relativity is the existence of gravitational waves (GWs) [25]. Einstein himself elucidated the theoretical existence of GWs as early as 1918 [26]. Today, however, GWs have still not been directly measured, although the measurements of the binary pulsar PSR1913+16 [27, 28, 29], (discovered by Hulse and Taylor and for which they won the Nobel prize) leave little doubt that GWs do, in fact, exist.

The fundamental factor that has led to our failure to directly measure GWs is the exceptional weakness of the gravitational coupling constant. This causes GWs to be too feeble to detect unless produced under extreme conditions. In particular, gravitational waves are produced by accelerating masses (a more exact formulation of this statement appears in 2.3). Thus, for the highest GW amplitudes, we seek sources with the highest possible accelerations and masses. As a result, astrophysical objects are the most plausible sources of GWs [3].

Further restrictions on viable sources are imposed by our detectors. For instance, for Earth based instruments, even with the best seismic isolation

[3] The exception to this statement is the big-bang itself, which should lead to a stochastic cosmological background of GWs, as mentioned in Sect. 1. LIGO has just begun to bound previously viable theoretical models of this background [11]. We will not be considering this background further in this review.

technologies currently available [30, 31], noise from seismic vibrations limits large-scale precision measurements to frequencies above about 30 Hz. Through causality, this time-scale limitation implies a maximum length-scale at the source of 10^3 km. Given the Chandrasekhar limit on the mass of a white dwarf star [32, 33] and the white dwarf mass-radius relationship this is somewhat less than the minimum length-scale for white dwarf stars [34].

Within the bounds of current knowledge, therefore, LIGO is limited to black holes and neutron stars as sources. According to our current understanding of astrophysical populations, these objects are relatively rare. Thus, the probability of finding them in our immediate stellar neighborhood are small, and any realistic search must be sensitive to these sources out to extragalactic distances to have a reasonable chance of seeing them in an observation time measured in years. Is this a reasonable prospect? The answer is yes, but to understand why, it behooves us to first understand a bit more about what GWs are and how they might be measured.

Gravitational waves arriving at Earth are perturbations of the geometry of space-time. Heuristically, they can be understood as fluctuations in the distances between points in space. Mathematically, they are modeled as a metric tensor perturbation $h^\alpha{}_\beta$ on the flat spacetime background. Linearizing the Einstein field equations of general relativity in $h^\alpha{}_\beta$, we find that this symmetric four-by-four matrix satisfies the the wave equation,

$$\left(-\frac{\partial^2}{\partial t^2} + c^2\nabla^2\right) h^\alpha{}_\beta \;=\; 8\pi\; G\; T^\alpha{}_\beta, \tag{1}$$

in an appropriate gravitational gauge. Here ∇^2 is the usual Laplacian operator, G is the gravitational constant, and $T^\alpha{}_\beta$ is the stress energy tensor, another symmetric four-by-four matrix which encodes information about the energy and matter content of the spacetime.

From (1), it is obvious that GWs travel at c, the speed of light. To understand the *production* of gravitational waves by a source, we solve (1) with the stress-energy ($T^\alpha{}_\beta$) of that source on the right-hand-side. We will discuss this in more detail in Sect. 2.3. First, however, we wish to consider the propagation of gravitational waves.

For the propagation of gravitational waves, we require solutions to the homogeneous ($T^\alpha{}_\beta = 0$) version of (1). As usual, such solutions can be expressed as linear combinations of the complex exponential functions

$$h^\alpha{}_\beta = A^\alpha{}_\beta \exp(\pm \mathrm{i} k_\mu x^\mu). \tag{2}$$

Here, $A^\alpha{}_\beta$ is a matrix of constant amplitudes, $k_\mu = (-\omega, \boldsymbol{k})$ is a four vector which plays the role of a wave vector in four dimensions, and $x^\mu = (t, \boldsymbol{x})$ are the spacetime coordinates. Above, and in what follows, we use the Einstein summation convention that repeated indices, such as the μ in $k_\mu x^\mu = -\omega t + \boldsymbol{k}\cdot\boldsymbol{x}$, indicates an implicit summation. It can be shown that for gauges in which (1) holds that

$$k_\mu h^\mu{}_\beta = 0. \tag{3}$$

In words, this means that the wave vector is orthogonal to the directions in which the GW distorts spacetime, i.e. the wave is transverse.

Since $h^\alpha{}_\beta$ is a four-by-four matrix, it has 16 components. However, because it is symmetric, only 10 of those components are independent. Further, (3) imposes four constraints on $h^\alpha{}_\beta$, reducing the number of free components to 6. One can use remaining gauge freedom to impose four more conditions on $h^\alpha{}_\beta$. There are therefore only two independent components of the matrix $h^\alpha{}_\beta$. Details can be found in any elementary textbook on General Relativity, such as [35].

The two independent components of $h^\alpha{}_\beta$ are traditionally called h_+ and $h_\times$. These names are taken from the effect that the components have on a ring of freely moving particles laying in the plane perpendicular to the direction of wave propagation, as illustrated in Fig. 1. The change in distance between

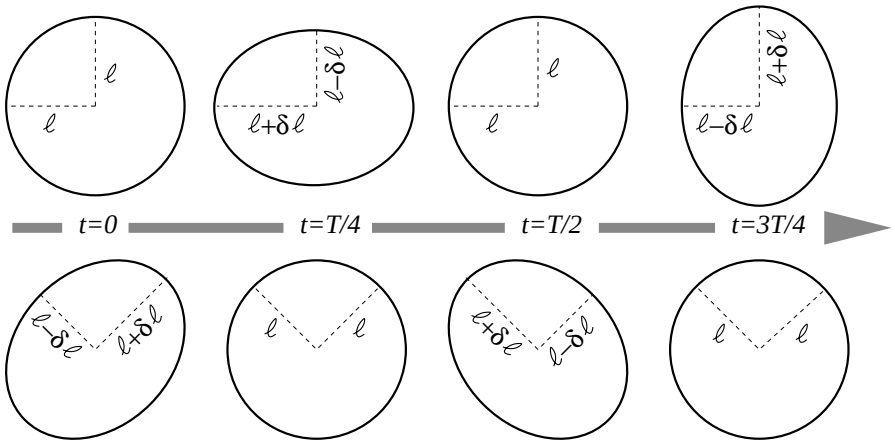

Fig. 1. Distortion of a ring of freely falling dust as a gravitational wave passes through. The wave is propagating into the page. From left to right are a series of four snapshots of the distortion of the ring. The top row are distortions due to h_+. The bottom row are distortions due to $h_\times$. The snapshots are taken at times $t = 0$, $t = T/4$, $t = T/2$ and $t = 3T/4$ respectively, where T is the period of the gravitational wave. The relative phase between h_+ and $h_\times$ corresponds to a circularly polarized gravitational wave.

particles, $\delta\ell$, is proportional to the original distance between them, ℓ, and the amplitude of the gravitational waves, $A^\alpha{}_\beta$. For a point source, which all astrophysical sources will effectively be, the amplitude decreases linearly with the distance from the source. For astrophysical source populations from which gravitational wave emission have been estimated, the typical gravitational wave strain, $h \sim 2\delta\ell/\ell$, at a detector at Earth would be expected to be less

than or of the order of 10^{-21} [36]. Through interferometry, it is possible to measure $\delta\ell \sim 10^{-18}$ m. Thus, interferometers of kilometer scales are required to have any chance of measuring these sources.

It might seem that the challenges in attempting to measure gravitational waves are so daunting as to call into question whether it is worthwhile at all. However, there are several factors which make the measurement of gravitational waves attractive. First, astrophysical gravitational wave sources include systems, such as black hole binaries, which are electromagnetically dark. Gravitational waves may therefore be the best way to study such sources. Second, since gravitation couples weakly to matter, gravitational waves propagate essentially without loss or distortion from their source to the detector. Thus, sources obscured by dust or other electromagnetically opaque media may still be observed with gravitational waves. Also, interferometers behave as amplitude sensing devices (like antennas), rather than energy gathering devices (like telescopes) for GWs, leading to a $1/r$ fall-off with distance, rather than the more usual $1/r^2$ fall-off [3].

But perhaps the most compelling reason for pursuing the measurement of gravitational waves is that they constitute an entirely new medium for astronomical investigation. History has demonstrated that every time a new band of the electromagnetic spectrum has become available to astronomers, it has revolutionized our understanding of the cosmos. What wonders, then, await us when we start to see the universe through the lens of gravitational waves, as we will surely begin to do within the next decade as our detectors continue their inevitable march toward higher sensitivities? Only time will tell, but there is every reason to be optimistic.

In this article, we concentrate on one of the many sources of gravitational waves for which searches are ongoing – binary neutron star (BNS) systems. In particular, LIGO's sensitive frequency band, which is approximately 40 Hz to 400 Hz, dictates that we should be interested in neutron star binaries within a few minutes of coalescence [37]. These sources hold a privileged place in the menagerie of gravitational waves sources LIGO is searching for. The Post-Newtonian expansion, a general relativistic approximation method which describes their motion, gives us expected waveforms to high accuracy [38, 39, 40]. They are one of the few sources for which such accurate waveforms currently exist, and they are therefore amenable to the most sensitive search algorithms available. Furthermore, while the population of neutron star binaries is not well understood, there are at least observations of this source with which to put some constraints on the population [41]. These two factor give BNS systems one of the best (if not the best) chance of discovery in the near future.

2.2 Gravitational Wave Detectors

Gravitational wave detectors have been in operation for over forty years now. However, it is only in the last five years or so that detectors with a non-negligible chance of detecting gravitational waves from astrophysical sources

have been in operation. The first gravitational wave detector to operate was built by Joseph Weber [42]. It consisted of a large cylinder of aluminum, two meters long and a meter in diameter, with piezoelectric crystals affixed to either end.

The fundamental idea for such detectors is that if a strong enough gravitational wave was to pass by, that it would momentarily reduce the interatomic distances, essentially compressing the bar, and setting it ringing, like a tuning fork. The ringing would create electric voltages in the piezoelectric crystals which could then be read off. Of course, as with a tuning fork, the response of the apparatus is greatly increased if it is driven at its resonant frequency (about 1660 Hz, for Weber's bars).

Weber's bar was isolated from seismic and electromagnetic disturbances and housed in a vacuum. He attributed the remaining noise to thermal motion of the aluminum atoms. This noise limited Weber's measurements to strains of $h{\sim}10^{-16}$, about five orders of magnitude less sensitive than the level now believed necessary to make the probability of detection non-negligible. Nonetheless, by 1969, Weber had constructed two bars and had observed coincident events in them although they were housed approximately 1000 miles apart. He calculated that his noise would create some of these events at rates as low as one per thousand years, and subsequently published his findings as "good evidence" for gravitational waves [43].

Many groups followed up on this and subsequent claims of gravitational wave detections made by Weber. No other group was ever able to reproduce these observations, and it is now generally agreed that Weber's events were spurious. Nonetheless, this launched the era of gravitational wave detectors, as resonant mass detectors (as Weber-like bars are now called) began operating in countries around the globe. Today, there is a network of these detectors operated under the general coordination of the International Gravitational Event Collaboration [44]. Technical advances have led to considerable improvements in sensitivity over the past decades. They continue to be rather narrow band detectors, however, and they are not the most sensitive instruments in operation today.

That distinction belongs to interferometric gravitational wave detectors [3]. The basic components of these detectors are a laser, a beam splitter to divide the laser light into two coherent beams, hanging mirrors to reflect the laser beams, and light sensing diode, as shown in Fig. 2. The mirrors act essentially as freely moving particles in the horizontal directions. If a sufficiently strong gravitational wave with a vertical component impinges, it shortens the distance between the beam splitter and one of the mirrors, and lengthens the distance between the beam splitter and the other mirror. This is registered as a shifting interference pattern by the light sensing diode, thus detecting the gravitational wave.

More specifically, what is measured is a quantity proportional to the strain on the detector, $s := (\delta x - \delta y)/\ell$, where δx and δy are the length changes in the two equal length arms of the interferometer, traditionally called the x

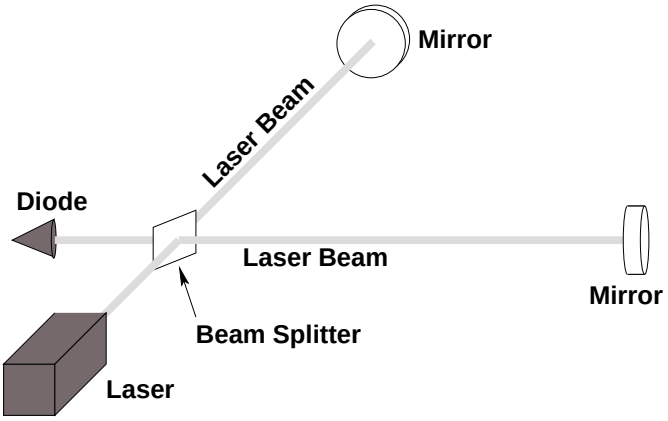

Fig. 2. Schematic diagram of an interferometric gravitational wave detector. The beam splitter is coated to allow half the light to be transmitted to one of the mirrors, and the other to be reflected to the other mirror. Real interferometric gravitational wave detectors are much more sophisticated, including frequency stabilization of the laser, a second mirror on each arm between the beam splitter and the end mirror to create Fabry-Perot cavities, and control feedback loops which "lock" the interferometer onto an interference fringe. Thus, rather than measuring the current from the photo-diode directly, the gravitational wave signals are encoded in the feedback loop voltages needed to maintain the lock of the interferometer. These and many other enhancements are necessary to reach the required sensitivity level.

and y arms, and ℓ is the unperturbed length of each arm. If there were no noise, then in the special case that h_+ or $h_\times$ was aligned with the arms, we would have $\delta x = \delta y = \delta\ell$ and the measured quantity would be proportional to $2\delta\ell/\ell$. For a more general alignment, but still in the absence of noise, some linear combination of h_+ and $h_\times$ is measured

$$h(t) \;:=\; F_+(\theta,\phi,\psi)\,h_+(t) + F_\times(\theta,\phi,\psi)\,h_\times(t), \tag{4}$$

where F_+ and $F_\times$ are called *beam pattern functions*. They project the gravitational wave components, h_+ and $h_\times$, onto a coordinate system defined by the detector, and are functions of the Euler angles (θ,ϕ,ψ) which relate this coordinate system to coordinates which are aligned with the propagating GW.

In the case where there is noise, δx and δy are sums of the gravitational wave displacements and the noise displacements, so that the detector strain is

$$s(t) = h(t) + n(t) \tag{5}$$

where $n(t)$ is the noise contribution. If the noise component can be kept from dominating the signal component, there is a reasonable chance that the gravitational wave can be detected. For a more complete and detailed account of interferometeric detection of gravitational waves, as well as many other aspects of gravitational wave physics, we recommend [36].

The idea of using an interferometer as a gravitational wave detectors was explored repeatedly but independently by several different researchers over approximately 15 years [45, 46, 47, 48]. The first prototype of an interferometric gravitational wave detector was built by one of Weber's students, Robert Forward, and collaborators in 1971 [49, 50]. The advantages of this idea were immediately understood, but, as mentioned above, an understanding also emerged that kilometer-scale interferometry would be needed. Thus, these detectors needed to be funded, built and operated as coordinated efforts at the national or international level.

To date, there have been six large-scale (100m plus) interferometers at operated at five sites. Three of the these are located in the United States and constitute the LIGO observatories – one four kilometer instrument at each of the LIGO-Hanford Observatory in Washington [51] and LIGO-Livingston Observatory in Louisiana [52] (H1 and L1 respectively), and a two kilometer instrument, housed in the same enclosure, at the LIGO-Hanford Observatory (H2). The other interferometers are the three kilometer Virgo instrument, located in Italy by a French-Italian collaboration [55], the German-English Observatory GEO600, a 600 meter interferometer in Germany [56], and the 300 meter TAMA observatory, located in and funded by Japan [57].

Other large-scale interferometers are in various stages of planning, although funding has not been secured for them. One of the most interesting is LISA, a planned joint NASA-ESA mission, which would consist of two independent million-kilometer-scale interferometers created by three satellites in solar orbit [58, 59]. The larger scale and freedom from seismic noise will make this instrument sensitive at much lower frequencies than its Earth-based brethren. This article will be primarily concerned with LIGO.

The Laser Interferometer Gravitational-wave Observatory (LIGO), began construction in 1994 and was commissioned in 1999. LIGO began taking scientific data on 23 August, 2002. That data taking run, called Science Run One (or S1 for short), ended 9 Sept., 2002. There have been four subsequent science runs: S2 from 14 Feb. to 14 Apr. 2003, S3 from 31 Oct. 2003 to 9 Jan. 2004, S4 from 22 Feb. to 23 Mar. 2005, and finally has been ongoing from S5 from Nov. 2005 and is expected to end in fall, 2007. At the conclusion of S5, the LIGO interferometers are scheduled for component enhancements which are expected to double the sensitivity of the instrument. The upgrade process is scheduled to last approximately a year.

Initial runs were short and periods between them were long because LIGO scientists and engineers were still identifying and eliminating technical and environmental noise sources which kept LIGO from running at its design sensitivity. As designed, LIGO sensitivity is expected to be bounded by three fundamental noise sources [48]. Below approximately 40 Hz, seismic noise transmitted to the mirrors through housing and suspension dominates. Between approximately 40 and 200 Hz, thermal vibrations in the suspension system for the mirrors dominates. Finally, above approximate 200 Hz, photon shot noise associated with counting statistics of the photons at the photodi-

ode. These three fundamental noise regimes, which contribute to the "noise floor" of LIGO, are described in the caption of Fig. 3.

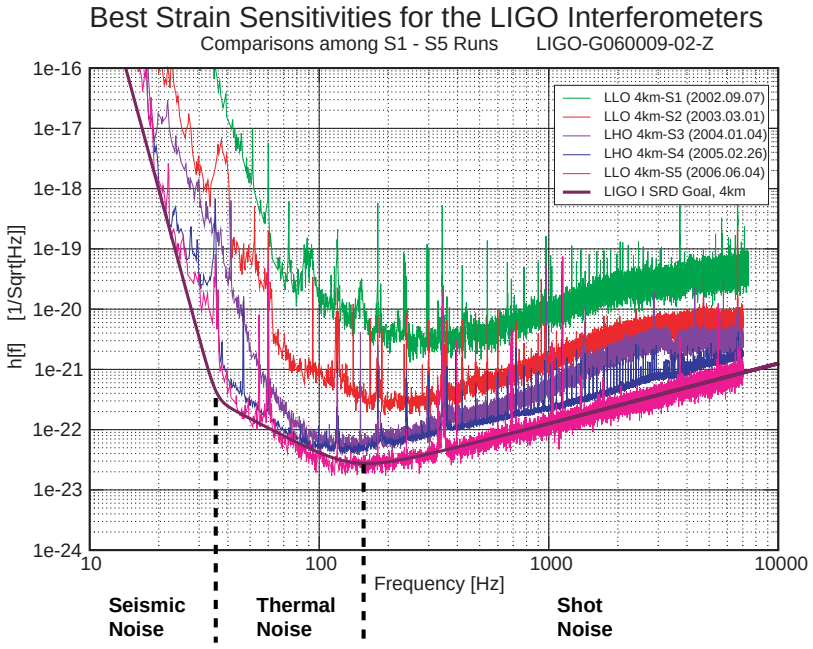

Fig. 3. Interferometer noise in each of the five science runs. The solid thick black curve is design goal of LIGO. There are two changes of slope indicated by dashed thick black lines. These correspond to changes in the dominant noise source – the three noise regimes are marked. Over four years of commissioning, the noise floor was reduced by approximately three orders of magnitude.

Apparent in Fig. 3 is the remarkable progress that has been made in lowering the noise floor and the other noises superimposed upon it in going from S1 to S5. Indeed, at S5, LIGO matches or exceeds its design specification over most frequency bands, including the most sensitive region from approximately 100–300 Hz. When S5 is over and S5 data is analyzed, it will provide by far the best opportunity to date to detect gravitational waves.

The degree to which improvements in the noise floor correspond to increase detection probabilities depend on the shape of the noise floor and the signal being sought. For neutron star binary inspiral signals, LIGO has devised a figure of merit called the inspiral range. This is the distance, averaged over all sky positions and orientations, to which a LIGO instrument can expect

to see a 1.4-1.4 $M_\odot$ binary with signal-to-noise ratio (defined below) of 8. For S2, typical inspiral ranges for L1 were just below 1 Mpc. For the LIGO design curve, the inspiral range is approximately 20 Mpc [60].

2.3 Neutron Star Binaries as Gravitational Wave Emitters

In the preceding subsections, we discussed the propagation and detection of gravitational waves. It is perhaps useful now to say a few words about the production of gravitational waves before diving into the particular sources of interest for this article, binary neutron star systems.

We have discussed solutions to the homogeneous ($T^\alpha{}_\beta = 0$) version of (1), which describe the propagation of GWs in the far wave zone. The generation of gravitational waves requires a source, and is therefore described by (1) with $T^\alpha{}_\beta \neq 0$. In fact, to lowest order, the relevant property of the source is the mass/energy density of the source, $\rho(t, \boldsymbol{x})$, or more specifically, the *mass quadrupole moments*.

The relevant moments depend on the direction from the source at which the gravitational wave is detected. In the limit of a negligibly gravitating source, the moments are given by the integrals

$$\mathcal{J}_+(t) := \frac{1}{2}\int \rho(t,\boldsymbol{x})\left[x^2 - y^2\right] d^3x, \tag{6}$$

$$\mathcal{J}_\times(t) := \int \rho(t,\boldsymbol{x})\, x\, y\, d^3x. \tag{7}$$

Here, $\boldsymbol{x} = \{x, y, z\}$ are Cartesian coordinates centered on the source with the z-axis being defined by the direction to the detector and t is time. In terms of these integrals, the relevant components of the solution to (1) with source is

$$h_+(t) = \frac{2}{r}\frac{G}{c^4}\frac{\partial^2}{\partial t^2}\mathcal{J}_+(t-r), \tag{8}$$

and likewise for $h_\times(t)$. Here r is the distance between the source and the detector.

While higher order multipole moments of the mass distribution can contribute to the radiation, for most systems the quadrupole will dominate. Further, the mass monopole and dipole moment will not contribute any gravitational waves. Thus, such events as a spherically symmetric gravitational collapse and axially symmetric rotation do not emit any gravitational radiation. On the other hand, a rotating dumbell is an excellent emitter of gravitational waves, making binary systems potentially amongst the brightest emitters of gravitational waves in the universe.

In general, the better the information about the gravitational wave signal, the better will be our chances of detecting it. This, in turn, prods us to find the best possible model of the dynamics of a GW emitting system. For the gravitational wave sources suitable for Earth-based interferometric detectors,

this proves to be difficult in general. For instance, the physics of core-collapse supernovae is not understood at the level of detail needed to accurately predict gravitational waveforms. This is also true of colliding black holes or neutron stars, which should emit large amounts of energy in gravitational waves. In fact there are only two sources for LIGO, the inspiral of binary neutron stars and intermediate mass ($\sim$100 $M_\odot$) perturbed black holes, for which the physics is well enough understood that it is believed that the waveforms calculated provided a high degree of confidence for detection[4].

Of these two potential sources, we at least know with great certainty that neutron star binaries, like the Hulse-Taylor binary, exist [41, 61, 62]. According to current thinking, these binaries are formed from the individual collapse of binaries of main sequence stars [63]. If one can establish a population model for our galaxy, therefore, one should be able to deduce the population outside the galaxy by comparing the rate of star formation in our galaxy to elsewhere. One measure of star formation is blue light luminosity of galaxies (corrected for dust extinction and reddening) [65, 64]. Thus, once a galactic population model is established, we can estimate the rate at which we can see gravitational waves from binary neutrons star (BNS) systems given a noise curve for our instrument.

To develop a population model, astrophysicists have used Monte Carlo codes to model the evolution of systems [67]. To cope with uncertainties in the evolutionary physics of these objects, a great many ($\sim$30) parameters must be introduced into the models, some of which can cause the predicted rates to vary by as much as two orders of magnitude. This can be reduced somewhat by feeding what is known about BNS systems from observation into the models [68]. However, only seven BNS systems have been discovered in the galactic disk. Furthermore, the most relevant for LIGO detection rates are the four BNS which are tight enough to merge within 10 Gyrs, since, as mentioned above, only those within minutes of merger are observable by LIGO. Thus, there is not much information to feed into these models, and estimates can still vary widely. The current best estimate is that LIGO should now be able to observe of the order of one BNS system every hundred years, although uncertainties extend this from a few per thousand years to almost one every ten years [63]. An improvement in LIGO's ability to detect BNS systems by a factor of three would therefore raise the most optimistic case to almost one BNS signal per year.

With projected rates this low, it is essential to search for BNS systems with the highest possible detection efficiency. Since, in general, the more in-

[4] To be fair, although the source mechanics of rotating neutron stars, like pulsars, are not well understood, the gravitational waves they produce if there is some asymmetry about the axis of rotation will be quasi-periodic. We therefore do not need to model these sources well to search for their gravitational waves. Similarly, although a stochastic background of gravitational waves in intrinsically unknowable in detail, a search for these waves can be optimized if their statistical properties are known.

formation that can be fed into the detection algorithm, the more efficient it will be, it is important to have a high accuracy theoretical prediction for the waveform. In the case of BNS systems, this prediction is provided by the restricted post-Newtonian approximation [38, 39, 40]. The post-Newtonian formalism uses an expansion in orbital velocity divided by c, the speed of light. Since this is a slow motion approximation, and the orbital velocity of the binary constantly increases during inspiral, this approximation becomes worse as the binary evolves. However, the accuracy is still good for BNS systems when they are in LIGO's band. Furthermore, we need only deal with circular orbits since initially eccentric orbits are circularized through the GW emission process [69]. Finally, one can safely ignore spin terms [70] and finite size effects [71]. Fig. 4 shows the post-Newtonian prediction for a neutron star binary in the sensitive frequency band of LIGO.

The general features of this waveform are easily understood. From (7), it is apparent that the mass quadrupole moment will be proportional to the square of the orbital radius, a^2. The second time derivative of this quadrupole moment therefore goes as $a^2\omega^2$, and from (8) we have that $h{\sim}a^2\omega^2$. For a Keplerian orbit, which relativistic orbits approximate when the Post-Newtonian approximation is valid, $\omega^2{\sim}a^{-3}$ and therefore $h{\sim}a^{-1}$. Thus, when the binary emits GWs, which carry of orbital energy, it experiences a progressive tightening, leading to an increased frequency and amplitude. If the two neutron stars are of equal mass, then the quadrupole configuration repeats itself every twice every orbital period, and the gravitational wave frequency is twice the orbital frequency. Because the two masses are comparable in every BNS system, the dominant frequency component is always at twice the orbital frequency.

3 Search Method

3.1 LIGO Data

As was mentioned in the caption of Fig. 2, LIGO interferometers are not the simple Michelson interferometers portrayed in that figure. Rather, they have a number of important and sophisticated refinements to that basic configuration, all designed to increase instrument sensitivity and reliability [3, 72]. For the purpose of understanding the data, the most important enhancement is that, when the IFOs are operational, their arm-lengths are held fixed, or *locked*. This is done by measuring the light at the antisymmetric port (the diode in Fig. 2) and applying feed-back controls to the mirrors through magnetic couplings [73, 74]. By measuring the feed-back loop voltage, it is possible to monitor how much the arm-lengths would have changed had the mirrors been free. This allows the suppression of pendulum modes which are either spurious or which might damage the optics if driven at resonance. The feedback control voltage is therefore the gravitational wave channel of the interferometer.

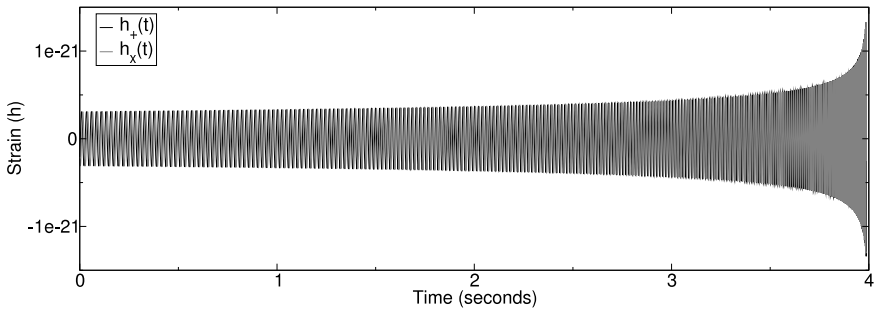

(a) Second-order restricted post-Newtonian waveforms from a 1.4–1.4 $M_\odot$ neutron star binary at 1 Mpc

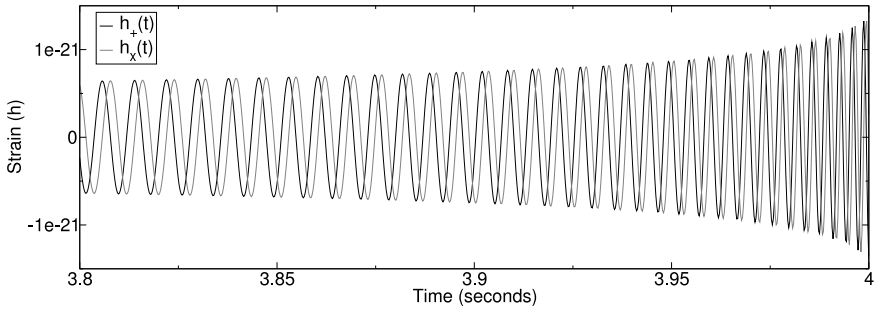

(b) Closeup of above waveforms

Fig. 4. Second-order restricted post-Newtonian h_+ and $h_\times$ waveforms from an optimally located and oriented 1.4–1.4 $M_\odot$ neutron star binary system at 1 Mpc. The top panel, (a), shows approximately the portion of the waveform visible to LIGO with frequency sweeping through $\sim$ 40–400 Hz. The bottom panel, (b), shows a closeup of the last 0.2 s of panel (a). From the closeup, we see that the waveforms are sinusoids sweeping upward in both frequency and amplitude as the binary companions inspiral toward one another. The two phases of the gravitational wave, h_+ and $h_\times$, are 90° out of phase. Thus, this is a circularly polarized gravitational wave.

This channel is sampled at 16384 Hz. In order to convert this voltage into detector strain, the frequency dependent transfer function between these two quantities must be applied. The overall shape of this transfer function in the frequency domain is determined by a model of the instrument, however, the overall scaling of the transfer function must be measured. This is done by driving the mirrors at specific frequencies and measuring the response in the control loop voltage [75]. At the frequencies at which these calibration signals are injected, one can see sharp line features in the noise spectra of the interferometers. These are some of the lines found in Fig. 3. Other lines are

caused by resonances in the wires suspending the mirrors. Lines at multiples of 60 Hz are caused by coupling of the electronic subsystems to the power grid mains. Fortunately, for the BNS search, these lines are not very problematic because the signal sweeps through frequencies and therefore never corresponds to one of these noisy frequencies for long.

As well as the gravitational wave channel, there are a myriad of channels monitoring the physical environment of the interferometer (seismic, magnetic, etc) and the internal status of the instrument (mirror alignment, laser power, etc). These can be used to veto epochs of gravitational wave data which are unreliable. Furthermore, since LIGO has three interferometers, all of which have similar alignment[5] and two of which are co-located, most false alarms can be eliminated by requiring coincidence of received signals in all interferometers.

Although the noise in LIGO is primarily Gaussian and stationary, there are occasional noise excursions, called *glitches*. The causes of some of these glitches are not apparent in the auxiliary channels. These constitute the primary source of background noise in the search for signals from neutron star binaries.

3.2 Matched Filtering and Chi-Squared Veto

When the expected signal is known in advance and the noise is Gaussian and stationary, the optimal linear search algorithm is *matched filtering* [76]. The idea behind matched filtering is to take the signal, and data segments of the same length as the signal, and treat them as members of a vector space. As with any two vectors in a vector space, the degree to which the signal and a data vector overlap is calculated using an inner product.

To be more precise, consider detector strain $s(t)$ and a signal $h(t)$ that lasts for a duration of T. If the signal arrives at the detector at time t_0, then the detector strain can be written

$$s(t) = \begin{cases} h(t-t_0) + n(t), & t_0 < t < t_0 + T \\ n(t), & \text{otherwise} \end{cases} \tag{9}$$

where $n(t)$ is the detector noise. For this paragraph, we will assume that, apart from being stationary and Gaussian, $n(t)$ is white (same average power at all frequencies) for simplicity. Then, the matched filter output, $\zeta(t)$, is given by

$$\zeta(t) = 2 \int_0^T h(\tau)\, s(t+\tau)\, d\tau. \tag{10}$$

At time $t = t_0$, we have

$$\zeta(t_0) = 2 \int_0^T h^2(\tau)\, d\tau + 2 \int_0^T h(\tau)\, n(t_0+\tau)\, d\tau. \tag{11}$$

[5] The detectors in Washington are somewhat misaligned with the detector in Louisiana due to the curvature of the Earth.

Let us denote the first and second integrals in (11) by I_1 and $I_2(t_0)$ respectively. Clearly, the integrand of I_1 is deterministic and positive everywhere. However, the integrand of I_2 is stochastic. The average of I_2 over all noise realizations vanishes. In other words, on average $\zeta(t_0) = I_1$ when there is a signal starting at time t_0. On the other hand, when there is no signal, $\zeta(t) = I_2(t)$. Denoting the standard deviation of I_2 over all noise realizations by σ, we define the *signal-to-noise ratio* (SNR) for the data to be

$$\varrho(t) := |\zeta(t)|/\sigma. \tag{12}$$

Clearly, at time t_0 the expected value of the SNR is $\varrho(t_0) = I_1/\sigma$. Thus, if the signal is strong enough that I_1 is several times larger than σ, there is a high statistical confidence that it can be detected.

In practice, it is preferable to implement the matched filter in the frequency domain. Thus, rather than a stretch of data $h(t)$, we analyze its Fourier transform

$$\tilde{h}(f) = \int_{-\infty}^{\infty} e^{-2\pi \mathrm{i} f t}\, h(t)\, dt, \tag{13}$$

where f labels frequencies. This has several advantages: first, it allows us to more easily deal with LIGO's non-white noise spectrum (cf. Fig. 3). Second, it allows us to use the stationary phase approximation to the restricted post-Newtonian waveform [36, 77], which is much less computationally intensive to calculate, and accurate enough for detection [78]. Third, it allows us to easily deal with one of the search parameters, the unknown phase at which the signal enters the LIGO band.

In the frequency domain, the matched filter is complex and takes the form

$$z(t) = x(t) + iy(t) = 4\int_0^{\infty} \frac{\tilde{s}^*(f)\tilde{h}(f)}{S_n(f)}\, e^{2\pi \mathrm{i} f t}\, df, \tag{14}$$

where $S_n(f)$ is the one-sided noise strain power spectral density of the detector and the $*$ superscript denotes complex conjugation. It can be shown that the variance of the matched filter due to noise is

$$\sigma^2 = 4\int_0^{\infty} \frac{\tilde{h}^*(f)\tilde{h}(f)}{S_n(f)}\, df. \tag{15}$$

In terms of $z(t)$, the SNR is given by

$$\varrho(t) = |z(t)|/\sigma. \tag{16}$$

Note that σ and $z(t)$ are both linear in their dependence on the signal template h. This means that the SNR is independent of an overall scaling of $h(t)$, which in turn means that a single template can be used to search for signals from the same source at any distance. Also, a difference of initial phase between the signal and the template manifests itself as a change in the complex phase

of $z(t)$. Thus, the SNR, which depends only on the magnitude of the matched filter output, is insensitive to phase differences between the signal and the template.

Equations (14-16) tell us how to look for a signal if we know which signal to look for. However, in practice, we wish to look for signals from any neutron star binary in the last minutes before coalescence. Because, as mentioned above, finite-size effects are irrelevant, a single waveform covers all possible equations of state for the neutron stars. Likewise, as stated above, the spinless waveform will find binaries of neutron stars with any physically allowable spin. Further, as just discussed, a single template covers all source distances and initial signal phases. However, a single template does not cover all neutron star binaries because it does not cover all masses of neutron stars.

Population synthesis models for neutron star binaries indicate that masses may span a range as large as $\sim$1–3 $\mathrm{M}_\odot$. Since mass is a continuous parameter, it is not possible to search at every possible mass for each of the neutron stars in the binaries. However, if a signal is "close enough" to a template, the loss of SNR will be small. Thus, by using an appropriate set of templates, called a *template bank*, one can cover all masses in the 1–3 $\mathrm{M}_\odot$ range with some predetermined maximum loss in SNR [79, 80]. The smaller the maximum loss in SNR, the larger the number of templates needed in the bank. LIGO has opted for a maximum SNR loss of 3%, which typically leads to template banks containing of the order of a few hundred templates (the exact number depends on the noise spectrum because both $z(t)$ and σ do, and therefore the number of templates can change from epoch to epoch).

If LIGO noise were stationary and Gaussian, then matched filtering alone would give the best probability of detecting a signal (given a fixed false alarm rate). However, as mentioned earlier, LIGO noise (and, indeed, all gravitational wave interferometer noise) contains noise bursts, or glitches, which provide a substantial noise background for the detection of binary inspirals. It is possible for strong glitches to cause substantial portions of the template bank to simultaneously yield high SNR values. It is therefore highly desirable to have some other way of distinguishing the majority of glitches from true signals.

The method that has become standard for this is to use a *chi-squared* (χ^2) veto [81]. When a template exceeds the trigger threshold in SNR, it is then divided into p different frequency bands such that each band should yield $1/p$ of the total SNR of the data if the high SNR event were a signal matching the template. The sum of the squares of the differences between the expected SNR and the actual SNR from each of the p bands, that is the χ^2 statistic, is then calculated. The advantage of using the χ^2 veto is that glitches tend to produce large (low probability) χ^2 values, and are therefore distinguishable from real signals. Thus, only those template matches with low enough χ^2 values are considered single detector triggers.

If the data were a matching signal in Gaussian noise, the χ^2 statistic would be χ^2 distributed with $2p-2$ degrees of freedom [81]. However, it is much more

likely that the template that produces the highest SNR will not be an exact match for the signal. In this case, denoting the fractional loss in SNR due to mismatch by μ, the statistic is distributed as a non-central chi-squared, with non-centrality parameter $\lambda \leq 2\varrho^2\mu$. This simply means that the χ^2 threshold, χ^*, depends quadratically on the measured SNR, ϱ, as well as linearly on μ.

In practice, the number of bins, p, and the parameters which relate the χ^2 threshold to the SNR , as well as the SNR threshold ϱ^* which an event must exceed to be considered a trigger are determined empirically from a subset of the data, the *playground data*. A typical playground data set would be ∼10% of the total data set, and would be chosen to be representative of the data set as a whole. Playground data is not used in the actual detection or upper limit analysis, since deriving search parameters from data which will be used in a statistical analysis can result in statistical bias. Values for these parameters for the LIGO S1 and S2 BNS analyses are given in Table 1.

Data Set	ϱ^*	p	L1 χ^*	H1/H2 χ^*
S1	6.5	8	$5\,(p + 0.03\varrho^2)$	$5\,(p + 0.03\,\varrho^2)$
S2	6.0	15	$5\,(p + 0.01\varrho^2)$	$12.5\,(p + 0.01\,\varrho^2)$

Table 1. Search algorithm parameters for S1 and S2 BNS searches. These parameters were determined using playground data extracted from the S1 and S2 data sets respectively. Note that the χ^2 threshold, χ^*, is different for the Louisiana and Washington instruments in the S2 run.

Finally, let us say a few words about clustering. As discussed earlier, when a glitch occurs, many templates may give a high SNR. This would also be true for a strong enough signal. It would be a misinterpretation to suppose that there might be multiple independent and simultaneous signals – rather, it is preferable to treat the simultaneous events as a cluster and then try to determine the statistical significance of that cluster as a whole. The simplest strategy, which has been used by LIGO thus far, is to take the highest SNR in the cluster and perform the χ^2 using the corresponding template. Another possibility might have been to take the lowest χ^2 value as the representative template, or some function of ϱ and χ^2. In fact, there is reason to believe that the last option may be best [23].

3.3 Coincidence and Auxiliary Channel Veto

Although the χ^2 veto reduces the rate of triggers from glitches, some glitch triggers survive. However, there are further tests that can be used to eliminate them. Because LIGO's three detectors are almost co-aligned, they should all be sensitive to the same signals (although the 2km H2 will only be half as sensitive to them as the 4km instruments). Thus, any signal that appears in

one should appear in all. On the other hand, there is no reason for glitches in one instrument to be correlated with glitches in another, especially between a detector located in Washington state and the Louisiana instrument. Thus, one way to distinguish between triggers generated by actual gravitational waves and those generated by glitches is to demand coincidence between triggers in different instruments.

The most fundamental coincidence is coincidence in time. The timing precision of the matched filtering in LIGO data is $\sim 1\,\mathrm{ms}$. The maximum time delay between the arrival of a gravitational wave at the Washington site and its arrival at the Louisiana site is 10 ms. Thus, triggers at one site which are not accompanied by triggers at the other site within 11 ms are likely not gravitational waves and can be discarded. There are several other quantities which should coincide between triggers in the three instruments. Of these, the only one which had been applied by LIGO to date as a trigger veto is the template which generated the trigger – the same template must have generated all coincident triggers (or represent all coincident clusters of triggers) or they are discarded.

The final hurdle that a trigger must overcome to remain viable is that it must not be associated with a known instrumental disturbance. Auxiliary channels which monitor the instruments and their environment contain information about many of the potential disturbances. Those channels most likely to correspond to spurious disturbances which would be manifest in the gravitational wave channel have been studied intensively. To date, studies have revealed no channel which allows for safe and useful auxilliary channel vetoes for the Washington instruments. However, for L1 it was discovered for the second science run that a channel which measures length fluctuations in a certain optical cavity of the interferometer had glitches which were highly correlated with glitches in the gravitational wave channel [82]. Thus, triggers which occurred within a time window 4 seconds earlier to 8 seconds later than a glitch in this auxiliary channel in Louisiana were also discarded.

Triggers which survive all of these cuts are examined individually to determine if they are genuine candidates for gravitational wave signals. The flow chart for the procedure we have just describe is shown in Fig. 5. A more comprehensive and detailed discussion of the algorithm can be found in [83]. In the next section, we discuss how the surviving candidates are analyzed and how upper limits are set from them.

4 Statistics and Results

4.1 Background

Once the method outlined above is completed, one is left with zero or more coincident triggers that need to be interpreted. The pipeline, and in particular the search parameters ϱ^* and χ^*, are chosen so that the probability of missing

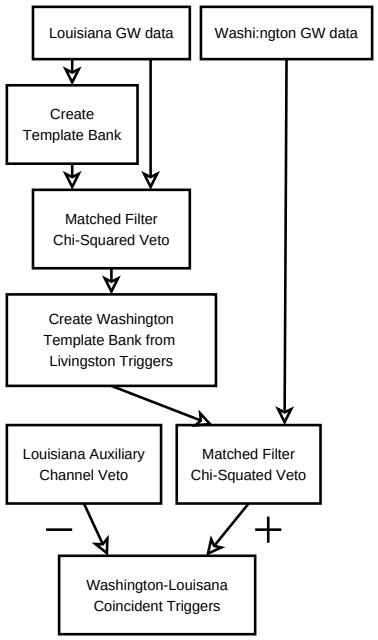

Fig. 5. A diagram showing the work-flow used by LIGO to look for signals from neutron star binaries for the second science run, S2. This is a two instrument work-flow involving one detector from Washington and the Louisiana detector. There is a slightly more complicated work-flow diagram when all three instruments are used. Note that the Washington data is only analyzed at times and for binary templates that correspond to a trigger in L1, thus minimizing both false alarms and computing time. The + and – signs by the two bottom-most arrows indicated that the addition and subtraction of coincident triggers respectively – i.e. passing the SNR and χ^2 thresholds adds coincident triggers, while occurring during an auxiliary channel glitch removes them.

a real signal are minimized. This means, in practice, that the probability of having coincident triggers from glitches is not minimized.

These coincident triggers from glitches form a *background* against which one does a statistical analysis to determine the likelihood that there are signals (foreground events). In order to accomplish this task, it is useful to understand the background rate. Ideally, one would have a model for the background, but there is no such model for LIGO glitches. However, there is a fundamental difference between background and foreground triggers that can be exploited – coincident background triggers are caused by random glitches which happened to coincide between detectors (assuming that the glitches in detectors are not correlated), where as foreground triggers are coincident because they are caused by the same gravitational wave signal. Thus, if one introduces an artificial time delay greater than 11 ms between the triggers from Louisiana

and those from Washington, the background rate should remain unchanged while the foreground rate must vanish [83, 83].

A large number of time shifts (40 for S2) are used to provide a great deal of background data and thus increase confidence in the inferred background rate. Both the mean and variance of the background rate are estimated. The foreground rate is then compared. If the foreground rate is significantly higher than the mean background rate, it is possible that some of the coincident triggers are from gravitational waves. A careful look at each coincident trigger then ensues. Criteria such as consistency of SNR values, problems with auxiliary channels, and behaviour of the gravitational wave channel are invoked to try to eliminate surviving background events. In particular, it is known that poor instrument behavior often leads to many consecutive glitches, and coincident triggers are much more likely during these glitchy times.

4.2 Upper Limits and the Loudest Event

If no gravitational wave candidate is identified amongst the coincident triggers, then the best one can do is set upper limits on the rate at which such signals occur. Clearly, it is meaningless to quote a rate unless we specify the minimum SNR we are considering. Since triggers can have different SNR's in each of the instruments, it is convenient to consider a measure of the combined SNR.

If the noise in all instruments were Gaussian, then it would be appropriate to combine SNR's in quadrature, $\varrho_C^2 = \varrho_H^2 + \varrho_L^2$, where ϱ_H and ϱ_L are the SNR's at Washington and Louisiana respectively. This would still be appropriate for non-Gaussian noise if the rate and SNRs of glitches were the same for instruments at both sites. However, this is not guaranteed to be the case, and if it is not, the noisier instrument can dominate the the upper limit statistics. To avoid this problem, the combined SNR needs to be modified slightly to

$$\varrho_C^2 = \varrho_H^2 + \alpha\varrho_L^2, \tag{17}$$

where α needs to be determined empirically.

Now, let us denote the mean rate at which signals arrive at LIGO detectors with SNR $\varrho_C > \varrho_C^*$ by $\mathcal{R}$. If we model the arrival of such signals as a Poisson process, then the probability of detecting such a signal within time T is given by

$$P(\varrho_C > \varrho_C^* \,;\, \mathcal{R}) = 1 - e^{\mathcal{R}T\varepsilon(\varrho_C^*)}, \tag{18}$$

where $\varepsilon(\varrho_C^*)$ is the detection efficiency, i.e. the ratio of detected signals to incident signals at the threshold ϱ_C^*. This is not the probability of observing a trigger with $\varrho_C > \varrho_C^*$ however, because it does not account for background triggers. If the probability of having no background event with $\varrho_C > \varrho_C^*$ is P_b, then the probability of observing at least one trigger with $\varrho_C > \varrho_C^*$ is

$$P(\varrho_C > \varrho_C^* \,;\, \mathcal{R}, b) = 1 - P_b\, e^{\mathcal{R}T\varepsilon(\varrho_C^*)}. \tag{19}$$

The loudest event (i.e. the event with the maximum combined SNR, $\varrho_{\max}$) sets the scale for the upper limit on the rate. More precisely, to find the 90% frequentist upper limit, one needs to determine the value of $\mathcal{R}$ such that there is a 90% chance that no combined SNR would exceed $\varrho_{\max}$ over the course of the run. In other words, one needs to solve $0.9 = P(\varrho_C > \varrho_{\max}\ ;\ \mathcal{R}, b)$ for $\mathcal{R}$. Doing so, we find

$$\mathcal{R}_{90\%} = \frac{2.303 + \ln P_b}{T\varepsilon(\varrho_{\max})}. \tag{20}$$

There are two quantities in (20) which need to be ascertained. The first is the efficiency of the detection algorithm to signals with combined SNR $\varrho_{\max}$. This is evaluated through Monte Carlo simulations where simulated signals from the target population of neutron star binaries (using the population models discussed in Sect. 2.3) are injected into the data.

The second is the background probability, P_b. The most straightforward approach might be to estimate it using the background events resulting from the timeshifts as described in Sect. 4.1. However, these background rates are known to be subject to significant variation depending on the details of search – e.g. reasonable changes to the event clustering criteria lead to different background rate estimates[23]. Since for detections one would follow up with detailed investigation of coincident triggers anyway, the background estimates are used in a more qualitative manner in this case, and this variation is not an issue. For an upper limit, however, we need a quantitative result for the background rates, and if there is uncertainty in the value obtained, it also must be quantified. Failing to do so could lead to undercoverage, i.e. a 90% upper limit which is below the actual rate that can be inferred from the data. Undercoverage is considered a "cardinal sin" in frequentist analyses.

Therefore, rather than try to get a quantitative estimate, LIGO has simply used $P_b = 1$ in (20). Note that this maximizes $\mathcal{R}_{90\%}$ with respect to P_b. It therefore gives a conservative upper limit – the actual 90% confidence rate is certainly lower. While undesirable, this is considered a "venial sin" in frequentist statistics, and therefore far preferable to undercoverage. Furthermore, since P_b is the probability that no background coincidences will occur with SNR above $\varrho_{\max}$, and since $\varrho_{\max}$ is the SNR of the loudest background coincidence that actually did occur, it is statistically unlikely that the actual $\mathcal{R}_{90\%}$ would be very much below the one obtained by this method. This statistic is known in LIGO as the *loudest event statistic*, and is discussed at some length in [86].

Finally, LIGO typically quotes BNS rate limits in units of "per Milky Way equivalent galaxy (MWEG) per year". This results from expressing the efficiency in terms of effective number of Milky Way equivalent galaxies to which the search was sensitive, N_G. The conversion between $\varepsilon(\varrho_{\max})$ and N_G is

$$N_G := \varepsilon(\varrho_{\max}) \left(\frac{L_{\text{pop}}}{L_G} \right), \tag{21}$$

where $L_{\rm pop}$ is the effective blue-light luminosity of the target population and $L_G = 9{\times}10^9\,L_\odot$ is the blue-light luminosity of the Milky Way galaxy. In terms of N_G, the 90% frequentist rate upper limit is written

$$\mathcal{R}_{90\%} = 2.303 \times \left(\frac{1\,\mathrm{yr}}{T}\right) \times \left(\frac{1}{N_G}\right) \mathrm{yr}^{-1}\mathrm{MWEG}^{-1}, \tag{22}$$

where T has units of years and $P_b = 1$ has been used. This, then, is the form of the upper limit that is quoted by LIGO and in this article.

4.3 Results

To date, LIGO has set to upper limits, based on S1 [24] and S2 [23] data, on the rate of binary neutron inspirals in its band. LIGO has also collaborated with TAMA for an additional upper limit[20]. No detections have been claimed for any analysis thus far. The results are summarized in Table 2.

Data Set	T (hrs)	N_G	$\mathcal{R}_{90\%}$ ($\mathrm{MWEG}^{-1}\mathrm{yr}^{-1}$)
LIGO S1	236	$0.60^{+0.12}_{-0.10}$	170
LIGO S2	339	$1.34^{+0.06}_{-0.07}$	47
LIGO/TAMA	584	$0.76^{+0.05}_{-0.06}$	49

Table 2. Results from three searches for neutron star binaries involving LIGO data. T is the observation time used for setting the upper limit, i.e. the total observation time minus playground data set length minus time periods lost due to vetoes. Note that the quoted rates are those given (22) when the lower bound for N_G is used, thus giving the most conservative upper limit.

All of these rates are substantially above the theoretically predicted rates for these searches[53]. Nonetheless, these are the best direct observational limits on neutron star binaries to date. Furthermore, even at these sensitivities, given how little is known about these gravitational wave sources, there is a real chance, however marginal, of a serendipitous discovery. Finally, however, the real impetus for performing these studies is to develop the analysis tools and methodologies that will maximize the possibility of discoveries in future analyses.

5 Future Prospects

5.1 LIGO Now and Future

As mentioned in the introduction, to date (Spring 2007), LIGO has completed four science runs, S1 from 23 Aug–9 Sep 2002, S2 from 14 Feb–14 Apr 2003,

S3 from 31 Oct 2003–9 Jan 2004, and S4 22 Feb– 23 Mar 2005. These short science runs were interspersed with periods of commissioning periods and have yielded dramatic improvements in sensitivity (see Fig. 3). LIGO is now operating with its design sensitivity. The fifth science run, S5, began in Nov 2005, and has the goal of collecting a full-year of coincident data at the LIGO design sensitivity. This goal is expected to be achieved by late summer 2007. The scientific reach of S5 – in terms of the product of the volume of the Universe surveyed times the duration of the data sample – will be more than two orders of magnitude greater than the previous searches.

A period of commissioning following the S5 run will hopefully improve the sensitivity of LIGO by a factor of ~ 2. An anticipated S6 run with the goal of collecting a year of data with this "enhanced" LIGO interferometer is projected to commence in 2009. If S6 sensitivity is indeed doubled, enhnaced LIGO will survey a volume eight times as great as the current LIGO sensitivity.

Following S6, in 2011, the LIGO interferometers are slated for decommissioning in order to install advanced interferometers. These advanced LIGO interferometers are expected to operate with 10 times the current sensitivity (a factor of 1000 increase in the volume of the Universe surveyed) by ~ 2014.

In addition to LIGO, the Virgo and GEO600 observatories are also participating in the S5 science run and are expected to undergo upgrades that will improve their sensitivity along with LIGO. Having several detectors operating at the time of a gravitational wave event allows better determination of the system's parameters.

5.2 Future Reach and Expected Rates

Since S2, a sequence of improvements to LIGO's sensitivity have been made (see Fig. 3) that have resulted in an order of magnitude increase in the range to which the inspiral searches are sensitive. Galaxy catalogs can be used to enumerate the nearby galaxies in which BNS inspirals could be detected. The relative contribution to the overall rate of BNS inspirals for each galaxy is determined by its relative blue light luminosity compared to that of the Milky Way. Monte Carlo methods are used to determine the fraction of BNS signals that would be detectable from each galaxy during a particular science run. As described above, this procedure yields a figure of merit of LIGO's sensitivity during any science run: the number of Milky Way Equivalent Galaxies (MWEG) that are visible to LIGO.

In the case of the second LIGO science run, S2, the search was sensitive to 1.34 MWEG. The S2 run produced a total of 339 hours (around 0.04 years) of analyzed data. The inverse of the product of the number of galaxies to which a search was sensitive times the livetime is a measure of the scientific reach of the search. For S2 this was $\sim 2\times 10^7\,\mathrm{Myr}^{-1}\,\mathrm{MWEG}^{-1}$. For initial LIGO sensitivity (which has been achieved during the current S5 science run) Nutzman et al. [54] estimate the effective number of MWEG surveyed to be

$\sim$600 MWEG, though this number depends on the actual sensitivity achieved during the search. Assuming that S5 produces one year of analyzed data, the scientific reach of this search is $\sim 2000\,\mathrm{Myr}^{-1}\,\mathrm{MWEG}^{-1}$. These numbers should be compared to estimated BNS merger rates in the Milky Way. For example, the "reference model" (model 6) of Kalogera et al. [53] quotes a Galactic rate of between $\sim$20 and $\sim 300\,\mathrm{Myr}^{-1}\,\mathrm{MWEG}^{-1}$ with a most likely rate of $\sim 80\,\mathrm{Myr}^{-1}\,\mathrm{MWEG}^{-1}$.

Extrapolating to the future, the enhancements that are expected to double the range of LIGO before the sixth science run could increase the scientific reach of LIGO to $\sim 200\,\mathrm{Myr}^{-1}\,\mathrm{MWEG}^{-1}$, which would now begin to probe the expected range of BNS coalescence rates. Since the Advanced LIGO is expected to improve the sensitivity by a factor of 10 compared to the current sensitivity, given a few years of operation a scientific reach of $\sim 1\,\mathrm{Myr}^{-1}\,\mathrm{MWEG}^{-1}$ should be achieved. It is therefore likely that detection of BNS inspirals will become routine during the operation of Advanced LIGO.

5.3 BNS Astrophysics with LIGO

As discussed above, we expect that future LIGO data runs will begin to probe the interesting range of BNS inspiral rates over the next several years; when Advanced LIGO begins running at its anticipated sensitivity, we expect BNS inspirals to be routinely detected, which will give a direct measurement of the true BNS merger rate as well as observed properties (such as the distribution of masses of the companions) of the population. Such constraints on the population of BNS can then be compared to the predictions from population synthesis models, which then can give insight into various aspects of the evolution of binary stars [68].

An intriguing possibility involves making measurements of neutron star equations of state using LIGO observations of BNS mergers. The advanced LIGO interferometers will be able to be tuned to optimize the sensitivity for a particular frequency band (while sacrificing sensitivity outside that band). This will give the ability to tune one of the LIGO interferometers to be most sensitive to gravitational waves at high frequencies, around 1 kHz, where effects due to the size of the neutron stars is expected to be imprinted in the gravitational waveform. Advanced LIGO could then make a direct measurement of the ratio of neutron star mass to radius and thereby constrain the possible neutron star equations of state [87].

Recent evidence suggests that short hard gamma-ray bursts (GRBs) could be associated with BNS mergers or neutron-star/black-hole binaries. A search for inspiral waveforms in conjunction with observed GRBs could confirm or refute the role of binaries as GRB progenitors if a nearby short GRB were identified. If the binary progenitor model is accepted then gravitational wave observations of the associated inspiral could give independent estimates or limits on the distance to the GRB. While most GRBs will be too distant for

us to hope to detect an associated inspiral, a few may occur within LIGO's range.

6 Concluding Remarks

We have reported here on recent result of LIGO's search for gravitational waves from neutron star binaries. No detections have been made in analyses published thus far, but this is hardly surprising given the gap between current sensitivities and those required to reach astrophysically predicted rates. Nonetheless, steady progress is being made in refining instrumentation and analyses in preparation for that time in the not-too-distant future when this gap has been closed.

It should be obvious to the reader that this is hardly a comprehensive description of any aspect of this search. Indeed, to provide such a description would require at least an entire volume to itself. Notably, our description of the mathematical theory of gravitational waves, the theoretical and computational underpinnings of population synthesis modeling and our discussion of interferometric design were all sketchy at best. Nor have we have not delved at all into the important topics of error analysis and pipeline validation at all.

Nonetheless, we have attempted to provide a birds-eye view of the relevant aspects with enough references to the literature to provide a starting point for readers interested in any particular aspect of these searches. And there is good reason to believe that, in time, gravitational wave searches will become increasingly interesting and relevant to a ever broadening group of astronomers and astrophysicists outside the gravitational wave community. Already, viable (if somewhat marginal) theoretical models have been constrained [11], and greater volumes of more sensitive data are in hand. It seems that it is only a matter of time before LIGO begins seeing the universe through gravitational waves. We look forward to the opportunity to report on the findings when it does.

Acknowledgements

We would like to thank Patrick Brady and Duncan Brown for their timely readings and comments on this manuscript. Our understanding and appreciation of gravitational wave physics has been enriched by our participation in the LIGO Scientific Collaboration, for which we are grateful. The writing of this article was supported by grant ¡+grant#+¿ from the National Science Foundation.

References

1. A. Abramovici et al: Science **256**, 325 (1992).

2. B. C. Barish, R. Weiss: Phys. Today **52** (Oct), 44 (1999).
3. P. R. Saulson: *Fundamentals of Interferometric Gravitational Wave Detectors* (World Scientic, Singapore 1994).
4. B. Abbott et al. (LIGO Scientific Collaboration), M. Kramer, A. G. Lyne: *Upper limits on gravitational wave emission from 78 radio pulsars* (2007),gr-qc/0702039.
5. B. Abbott et al. (LIGO Scientific Collaboration): *Coherent searches for periodic gravitational waves from unknown isolated sources and Scorpius X-1: Results from the second LIGO science run* (2006), gr-qc/0605028.
6. B. Abbott et al. (LIGO Scientific Collaboration): Phys. Rev.D **72**, 102004 (2005).
7. B. Abbott et al. (LIGO Scientific Collaboration): Phys. Rev. Lett. **94**, 181103 (2005).
8. B. Abbott et al. (LIGO Scientific Collaboration): Phys. Rev. D **69**, 082004 (2004).
9. B. Abbott et al. (LIGO Scientific Collaboration and Allegro Collaboration): *First cross-correlation analysis of interferometric and resonant-bar gravitational-wave data for stochastic backgrounds* (2007), gr-qc/0703068.
10. B. Abbott et al. (LIGO Scientific Collaboration): *Upper limit map of a background of gravitational waves* (2007), stro-ph/0703234.
11. B. Abbott et al. (LIGO Scientific Collaboration): *Searching for a stochastic background of gravitational waves with LIGO* (2006), astro-ph/0608606.
12. B. Abbott et al. (LIGO Scientific Collaboration): Phys. Rev. Lett. **95**, 221101 (2005).
13. B. Abbott et al. (LIGO Scientific Collaboration): Phys. Rev. D **69**, 122004 (2004).
14. B. Abbott et al. (LIGO Scientific Collaboration): *Search for gravitational wave radiation associated with the pulsating tail of the SGR 1806-20 hyperflare of 27 December 2004 using LIGO* (2007),astro-ph/0703419.
15. B. Abbott et al. (LIGO Scientific Collaboration): Class. Quant. Grav. **23**, S29-S39 (2006).
16. B. Abbott et al. (LIGO Scientific Collaboration), T. Akutsu et al. (TAMA Collaboration): Phys. Rev. D **72**, 122004 (2005).
17. B. Abbott et al. (LIGO Scientific Collaboration): Phys. Rev. D **72**, 062001 (2005).
18. B. Abbott et al. (LIGO Scientific Collaboration): Phys. Rev. D **72**, 042002 (2005).
19. B. Abbott et al. (LIGO Scientific Collaboration): Phys. Rev. D **69**, 102001 (2004).
20. B. Abbott et al. (LIGO Scientific Collaboration), T. Akutsu et al. (TAMA Collaboration): Phys. Rev. D **73**, 102002 (2006).
21. B. Abbott et al. (LIGO Scientific Collaboration): Phys. Rev. D *73*, 062001 (2006).
22. B. Abbott et al. (LIGO Scientific Collaboration): Phys. Rev. D **72**, 082002 (2005).
23. B. Abbott et al. (LIGO Scientific Collaboration): Phys. Rev. D **72**, 082001 (2005).
24. B. Abbott et al. (LIGO Scientific Collaboration): Phys. Rev. D **69**, 122001 (2004).

25. A. Einstein: Sitzungsberichte der Königlich Preussischen Akademie der Wissenschaften Berlin, 688696 (1916).
26. A. Einstein: Sitzungsberichte der Königlich Preussischen Akademie der Wissenschaften Berlin, 154167 (1918).
27. J. H. Taylor, J. M. Weisberg: Astrophys. J. **253**, 908 (1982).
28. J. H. Taylor, J. M. Weisberg: Astrophys. J. **345**, 434 (1989).
29. J. M. Weisberg, J. H. Taylor: in *Radio Pulsars*, ed by M. Bailes, D. J. Nice, S. Thorsett (ASP. Conf. Series, 2003).
30. J. Giaime, P. Saha, D. Shoemaker, L. Sievers: Rev. Sci. Inst. **67**, 208 (1996).
31. J. Giaime, E. Daw, M. Weitz, R. Adhikari, P. Fritschel, R. Abbott, R. Bork, J. Heefner: Rev. Sci. Inst. **74**, 218 (2003).
32. S. Chandrasekhar: MNRAS **91**, 456 (1931).
33. S. Chandrasekhar: MNRAS **95**, 207 (1935).
34. J. L. Provencal, H. L. Shipman, E. Høg, P. Thejll: Astrophys. J. **494**, 759 (1998).
35. B. F. Schutz: *A First Course in General Relativity* (Cambridge University Press, 1985).
36. K. S. Thorne: in *300 Years of Gravitation*, ed by S. W. Hawking, W. Israel (Cambridge University Press, 1987).
37. C. Cutler et al: Phys. Rev. Lett. **70**, 2984 (1993).
38. L. Blanchet, T. Damour, B. R. Iyer, C. M. Will, A. G. Wiseman: Phys. Rev. Lett. **74**, 3515 (1995).
39. L. Blanchet, B. R. Iyer, C. M. Will, A. G. Wiseman: Class. Quant. Grav. **13**, 575 (1996).
40. T. Damour, B. R. Iyer, B. S. Sathyaprakash: Phys. Rev. D **63**, 044023 (2001).
41. I. H. Stairs: Science **304**, 547 (2004).
42. J. Weber: Phys. Rev. Lett. **20**, 1307 (1968).
43. J. Weber: Phys. Rev. Lett. **22**, 1320 (1969).
44. Z. A. Allen et al. (International Gravitational Event Collaboration): Phys. Rev. Lett. **85**, 5046 (2000).
45. F.A.E. Pirani: Acta Physica Polonica **15**, 389 (1956).
46. M. E. Gertsenshtein, V. I. Pustovoit: Sov. Phys. JETP **14**, 433 (1962).
47. J. Weber: unpublished.
48. R. Weiss: Quarterly Progress Report of the Research Laboratory of Electronics of the Massachusetts Institute of Technology **105**, 54 (1972).
49. G.E. Moss, L.R. Miller, R.L. Forward: Appl. Opt. **10**, 2495 (1971).
50. R.L. Forward: Phys. Rev. D **17**, 379 (1978).
51. See `http://www.ligo-wa.caltech.edu/`.
52. See `http://www.ligo-la.caltech.edu/`.
53. V. Kalogera et al: Astrophys. J. **601**, L179 (2004). [Erratum: ibid. **614**, L137 (2004)].
54. P. Nutzman, V. Kalogera, L. S. Finn, C. Hendricksen, K. Belczynski: Astrophys. J. **612**, 364 (2004).
55. F. Acernese et al. (Virgo Collaboration): Class. Quant. Grav. **19**, 1421 (2002).
56. B. Willke et al. (GEO): Class. Quant. Grav. **19**, 1377 (2002).
57. H. Tagoshi et al. (TAMA): Phys. Rev. D **63**, 062001 (2001).
58. See `http://lisa.nasa.gov/`.
59. See `http://www.esa.int/esaSC/120376_index_0_m.html`.
60. L. S. Finn: in *Astrophysical Sources For Ground-Based Gravitational Wave Dectectors*, ed by J. M. Centrella (Amer. Inst. Phys., Melville, N.Y., 2001), gr-qc/0104042.

61. R. A. Hulse: Rev. Mod. Phys. **66**, 699 (1994).
62. J. H. Taylor: Rev. Mod. Phys. **66**, 711 (1994).
63. V. Kalogera, K. Belczynski, C. Kim, R. OShaughnessy, B. Willems: *Formation of Double Compact Objects*, (2006) astro-ph/0612144.
64. V. Kalogera, R. Narayan, D. N. Spergel, J. H. Taylor: Astrophys. J. **556**, 340 (1991).
65. E. S. Phinney: Astrophys. J. **380**, L17 (1991).
66. K. Belczynski, V. Kalogera, T. Bulik: Astrophys. J. **572**, 407 (2002).
67. K. Belczynski et al: *Compact Object Modeling with the StarTrack Population Synthesis Code*, 2005 astro-ph/0511811.
68. R. O'Shaughnessy, C. Kim, V. Kalogera, K. Belczynski: *Constraining population synthesis models via observations of compact-object binaries and supernovae*, (2006) astro-ph/0610076.
69. P. C. Peters: Phys. Rev. **136**, B1224 (1964).
70. T. A. Apostolatos: Phys. Rev. D **52**, 605 (1995).
71. L. Bildsten, C. Cutler: Astrophys. J. **400**, 175 (1992).
72. B. Abbott et al. (LIGO Scientic Collaboration): Nucl. Instrum. Methods **A517**, 154 (2004).
73. P. Fritschel et al: Appl. Opt. **37**, 6734 (1998).
74. P. Fritschel et al: Appl. Opt. **40**, 4988 (2001).
75. R. Adhikari, G. González, M. Landry, B. OReilly: Class. Quant. Grav. **20**, S903 (2003).
76. L. A. Wainstein, V. D. Zubakov: *Extraction of signals from noise* (Prentice-Hall, Englewood Cliffs, NJ, 1962).
77. B.S. Sathyaprakash, S.V. Dhurandhar: Phys. Rev. D **44**, 3819 (1991) .
78. S. Droz, D. J. Knapp, E. Poisson, B. J. Owen: Phys. Rev. D **59**, 124016 (1999).
79. B. J. Owen: Phys. Rev. D **53**, 6749 (1996).
80. B. J. Owen, B. S. Sathyaprakash: Phys. Rev. D **60**, 022002 (1999).
81. B. Allen: Phys. Rev. D **71**, 062001 (2005).
82. N. Christensen, P. Shawhan, G. González: Class. Quant. Grav. **21**, S1747 (2004).
83. E. Amaldi et al: Astron. Astrophys. **216**, 325 (1989)
84. P. Astone et al: Phys. Rev. D **59**, 122001 (1999).
85. B. Allen, W. G. Anderson, P. R. Brady, D. A. Brown, J. D. E. Creighton: *FINDCHIRP: An algorithm for detection of gravitational waves from inspiraling compact binaries*, (2005) gr-qc/0509116.
86. P. R. Brady, J. D. E. Creighton, A. G. Wiseman: Class. Quant. Grav. **21**, S1775 (2004).
87. J. A. Faber, P. Grandclément, F. A. Rasio, Phys. Rev. Lett. **89**, 231102 (2002).